Copy 6
RM A51C14

NACA RM A51C14

NACA

RESEARCH MEMORANDUM

A SEMIEMPIRICAL METHOD FOR CALCULATING THE PITCHING MOMENT OF BODIES OF REVOLUTION AT LOW MACH NUMBERS

By Edward J. Hopkins

Ames Aeronautical Laboratory
Moffett Field, Calif.

NATIONAL ADVISORY COMMITTEE
FOR AERONAUTICS

WASHINGTON
May 17, 1951

NATIONAL ADVISORY COMMITTEE FOR AERONAUTICS

RESEARCH MEMORANDUM

A SEMIEMPIRICAL METHOD FOR CALCULATING THE PITCHING MOMENT OF BODIES OF REVOLUTION AT LOW MACH NUMBERS

By Edward J. Hopkins

SUMMARY

A semiempirical method is presented for calculating the pitching moments and forces for bodies of revolution inclined at moderate angles of attack at low Mach numbers. In this method the transverse forces on a forward portion of the body are calculated from potential-flow considerations. The transverse forces on the remaining portion of the body are estimated by relating the local transverse force for the inclined body to the drag force for a circular cylinder in a manner similar to that used in NACA RM A9I26, 1949. However, this somewhat arbitrary procedure of employing the cylinder-drag force only over the rearward portion of the body differs from the approximate method given in NACA RM A9I26 in which the cylinder-drag forces are added to the transverse forces derived from potential-flow considerations along the entire length of the body. For the method presented herein, an empirically derived curve based upon experimental pitching-moment results is given from which an estimate can be made of the portion of the body for which potential theory should be applied.

The lift, drag, and pitching-moment characteristics of 15 bodies of revolution with fineness ratios ranging from 4.0 to 12.5 were calculated by the method of this report, by the method of NACA RM A9I26, and by potential theory. The results of these calculations are compared with experimental data. The pitching moments calculated by the method of this report gave the best agreement with the experimental data for nearly all the bodies. The agreement with the experimental lift and drag characteristics as given by the method of this report was generally as good as that given by NACA RM A9I26.

INTRODUCTION

One of the first attempts to utilize potential theory for the estimation of the aerodynamic forces and moments for bodies of revolution

was made by Munk in connection with his work on airships (reference 1). Several other investigators have developed similar methods which give essentially the same results (references 2 and 3). It has been shown (references 4 and 5) that for the expanding portion of the body at an angle of attack these methods give an accurate prediction of the transverse forces. However, for the contracting portion of the body where the effects of viscosity become important, the predicted transverse forces do not agree with experiment. In reference 6 an approximate theory to account for the effects of viscosity was developed for inclined bodies of revolution. This approximate theory results in satisfactory agreement between the predicted and experimental lift and drag forces. However, the agreement between the experimental and theoretical pitching moments is not as favorable, since the longitudinal distribution of the transverse load is not accurately represented by the method of reference 6.

The purpose of the present investigation was to combine the potential theory and the viscous cross-flow theory in a manner which would permit a more accurate prediction of the low-speed pitching moments of bodies of revolution. The semiempirical method thus derived is also applied to the prediction of the lift and drag forces.

NOTATION

C_D drag coefficient $\left(\frac{\text{drag}}{q(V)^{2/3}}\right)$

ΔC_D increase in body drag coefficient above that at an angle of attack of zero degrees

c_{d_c} section drag coefficient of a circular cylinder normal to air stream $\left(\frac{\text{drag/unit length}}{2qr}\right)$
(See fig. 1 for data taken from references 7 to 10.)

C_L lift coefficient $\left(\frac{\text{lift}}{q(V)^{2/3}}\right)$

C_m pitching-moment coefficient $\left(\frac{\text{pitching moment}}{qV}\right)$

$k_2 - k_1$ difference between the transverse and longitudinal apparent mass coefficients
(See fig. 2 for data taken from reference 11.)

[redacted]

L	body length, feet
n	fineness ratio $\left(\frac{L}{2r_o}\right)$
q	free-stream dynamic pressure, pounds per square foot
r	local body radius, feet
r_o	maximum body radius, feet
R_c	cross Reynolds number $\left(\frac{2r V_o \sin \alpha}{\nu}\right)$
S	cross-sectional area normal to the longitudinal axis of a body at any longitudinal station, square feet
V	body volume, cubic feet
V_o	free-stream velocity, feet per second
x	longitudinal distance from body nose, feet
x_1	longitudinal distance from body nose to point at which dS/dx has a maximum negative value, feet
x_m	longitudinal distance from body nose to moment axis, feet
x_o	longitudinal distance from body nose over which potential-flow theory is used in the method of this report
α	angle of attack, degrees or radians
ν	kinematic viscosity, feet squared per second
η	ratio of the drag coefficient of a circular cylinder of finite length to that for a cylinder of infinite length (See fig. 3 for data taken from reference 12.)

ANALYSIS

A study of the low-speed pressure distribution of two inclined bodies with greatly different nose contours (models 1 and 13 of fig. 4) indicated that the transverse forces acting on the expanding portions of

these bodies agreed well with those predicted by potential theory. However, for the contracting portions of these bodies where the effects of viscosity become more important, the transverse forces predicted by potential theory did not agree with experiment (see references 4 and 5). It was reasoned, therefore, that one possible method for obtaining good agreement between the predicted and experimental pitching moments would be to assume potential flow over only a forward portion of the body and viscous flow for the remainder of the body. The viscous cross flow, similar to that experienced on a circular cylinder in a real fluid, was assumed in a manner parallel to that used in reference 6. These assumptions differ from those made in reference 6 in which the viscous cross force was added to the transverse force given by potential theory at each longitudinal station.

The pitching-moment, lift, and drag coefficients can be expressed in equation form[1] for the method of this report as follows:

$$C_m = \frac{(k_2-k_1)2\alpha}{V}\int_0^{x_0} \frac{dS}{dx}(x_m-x)\,dx + \frac{2\alpha^2}{V}\int_{x_0}^{L} \eta\, r\, c_{d_c}\,(x_m-x)\,dx \qquad (1)$$

$$C_L = \frac{(k_2-k_1)2\alpha}{(V)^{2/3}}\int_0^{x_0} \frac{dS}{dx}\,dx + \frac{2\alpha^2}{(V)^{2/3}}\int_{x_0}^{L} \eta\, r\, c_{d_c}\,dx \qquad (2)$$

$$C_D = \frac{(k_2-k_1)2\alpha^2}{(V)^{2/3}}\int_0^{x_0} \frac{dS}{dx}\,dx + \frac{2\alpha^3}{(V)^{2/3}}\int_{x_0}^{L} \eta\, r\, c_{d_c}\,dx \qquad (3)$$

The factors c_{d_c}, k_2-k_1, and η (assumed to be a function of the fineness ratio of a full-length body) may be found in figures 1, 2, and 3, respectively. The angle of attack, α, is measured in radians.

The above equations are similar to those given in reference 6 with the following exceptions:

1. The limits of integration differ from those given in reference 6. The first term of each equation (the term given by potential theory) is

[1]Because of the empirical nature of the method, equations (1), (2), and (3) are given in simplified form for which the following assumptions have been made: (a) Cosines of angles have been replaced by unity and sines of angles, by angles in radians. (b) The lift component of the viscous axial force has been neglected in equation (2) because the inclusion of this component would change the total lift a negligible amount.

integrated only to x_o, the distance determined from an empirically derived relation given in figure 5 which will be discussed hereinafter. The second term of the equations (the term derived from cylinder drag considerations) is integrated only over the remainder of the body from x_o to the tail end.

2. The first term of equation (3) is greater by a factor of 2 than the corresponding term of the equation for drag coefficient given in reference 6. The change was introduced by differences in the derivation. This term of the equation given herein was derived by considering the drag increment from potential theory to be equal to the transverse force given by Munk in reference 1 multiplied by the angle of attack. This was found to be a good approximation by comparing the product of the experimental lift coefficient and the angle of attack (in radians) with the increment of experimental drag coefficient shown in figure 6 for the 15 bodies of revolution.

Experimental data for 15 bodies of revolution were analyzed throughout the angle-of-attack range from 0° to 20° to determine the portion of the body for which potential theory should be employed to attain optimum agreement between the calculated and experimental pitching moments. Sketches and pertinent dimensional data for the models used in the analysis (obtained from references 13 through 20 and unpublished data) are presented in figure 4 and table I. It was found that the longitudinal distance x_o (the limit of integration in equations (1), (2), and (3)) could be correlated with the longitudinal station on the body at which the rate of change of cross-sectional area with longitudinal distance has a maximum negative value. The results of this correlation are shown in figure 5 with the computed line of regression. This line of regression is defined as a line for which the sum of the squares of the deviations (the differences between the line and the individual points) is a minimum. It will be shown that by use of this line of regression satisfactory agreement can be obtained between calculated and experimental pitching moments. The equation for the line of regression in figure 5 is

$$\frac{x_o}{L} = 0.378 + 0.527 \frac{x_1}{L} \tag{4}$$

RESULTS AND DISCUSSIONS

The experimental lift, drag, and pitching-moment coefficients for 15 bodies of revolution are compared with the characteristics calculated by the method of this report in figure 6. For the calculations, equation (4) was used to determine x_o/L. Also, to simplify the calculations

a constant value of cylinder drag coefficient of 1.2 was used, as the cross Reynolds numbers for the rearward portions of the bodies were less than the critical Reynolds number for a circular cylinder. The characteristics calculated by the method of reference 6 and by potential theory are also shown in figure 6.

The pitching-moment coefficients calculated by the method proposed herein are in closest agreement with the experimental data, for the moment reference centers shown in figure 6, with the exception of the data for model 14. These moment centers correspond to those for which the experimental data were presented in references 13 to 20. Both potential theory and the method of reference 6 tend to overestimate the pitching-moment coefficients. The method proposed herein appears to give the best agreement with the slope of the experimental pitching-moment curve at the lower angles of attack. It is possible that better agreement could have been realized at the higher angles of attack provided that x_o had been allowed to move forward along the body with increasing angle of attack.

The method proposed herein, in general, gives as good agreement with the experimental lift and drag coefficients as the method of reference 6. This evidence is not sufficient, however, to indicate which of these two methods gives the best agreement with the lift and drag characteristics for specific types of bodies.

To indicate the relative contribution of each part of the equations for lift and pitching-moment coefficient, the potential terms of equations (1) and (2) were calculated and the results are also shown in figure 6. It can be seen that the contribution of the potential term is the major part of the total for lift and for pitching-moment coefficient.

The potential term of equation (1) for pitching-moment coefficient can be considered as consisting of a moment coefficient due to lift and a moment coefficient due to a couple. These moment coefficients were calculated and the results are presented in figure 7 for models 1 and 5, which have greatly different nose contours and fineness ratios. It should be noted that the largest portion of the calculated pitching-moment coefficient is derived from the moment couple which is independent of moment-reference center.

An indication of the adequacy of representation of the longitudinal distribution of load by the method of this report can be obtained by considering the pitching-moment coefficients given in figure 6 about a different moment-reference center. Therefore, the calculated and experimental pitching-moment coefficients for all the models are shown in figure 8 with the moment-reference centers transferred 0.25L from the locations given in figure 6. This transfer does not affect the agreement

of moments predicted by the proposed method with the experimental data, except for model 9 for which the method of reference 6 is shown to give the better agreement. These comparisons indicate that the longitudinal distribution of load proposed in this report, although based on an arbitrary combination of potential theory and viscous cross-flow theory, results in improved accuracy for calculating the low-speed pitching-moment coefficients for inclined bodies of revolution.

Ames Aeronautical Laboratory,
National Advisory Committee for Aeronautics,
Moffett Field, Calif.

REFERENCES

1. Munk, Max M.: The Aerodynamic Forces on Airship Hulls. NACA Rep. 184, 1924.

2. Upson, Ralph H., and Klikoff, W. A.: Application of Practical Hydrodynamics to Airship Design. NACA Rep. 405, 1931.

3. Laitone, E. V.: The Linearized Subsonic and Supersonic Flow About Inclined Bodies of Revolution. Jour. Aero. Sci., vol. 14, no. 11, Nov. 1947, pp. 631-642.

4. Freeman, Hugh B.: Pressure-Distribution Measurements on the Hull and Fins of a 1/40-Scale Model of the U.S. Airship "Akron." NACA Rep. 443, 1932.

5. Allen, H. Julian: Pressure Distribution and Some Effects of Viscosity on Slender Inclined Bodies of Revolution. NACA TN 2044, 1950.

6. Allen, H. Julian: Estimation of the Forces and Moments Acting on Inclined Bodies of Revolution of High Finess Ratio. NACA RM A9I26, 1949.

7. Lindsey, W. F.: Drag of Cylinders of Simple Shapes. NACA Rep. 619, 1938.

8. Stack, John: Compressibility Effects in Aeronautical Engineering. NACA ACR, Aug. 1941.

9. Wieselsberger, C.: New Data on the Laws of Fluid Resistance. NACA TN 84, 1922.

[redacted]

10. Relf, E. F.: Discussion of the Results of Measurements of the Resistance of Wires, with Some Additional Tests on the Resistance of Wires of Small Diameter. R.&M. No. 102, British A.C.A., Mar. 1914.

11. Lamb, Sir Horace: Hydrodynamics. Dover Publications, N.Y., 1945, p. 155.

12. Goldstein, S., ed.: Modern Developments in Fluid Dynamics. Oxford, The Clarendon Press. Vol. 2, sec. 195, 1938, pp. 439–440.

13. Jones, J. Lloyd and Demele, Fred A.: Aerodynamic Study of a Wing–Fuselage Combination Employing a Wing Swept Back 63° – Characteristics Throughout the Subsonic Speed Range with the Wing Cambered and Twisted for a Uniform Load at a Lift Coefficient of 0.25.. NACA RM A9D25, 1949.

14. Hoggard, H. Page, Jr.: Wind-Tunnel Investigation of Fuselage Stability in Yaw with Various Arrangements of Fins. NACA TN 785, 1940.

15. Lange, G.: Force and Pressure-Distribution Measurements on Eight Fuselages. NACA TM 1194, 1948.

16. Jacobs, Eastman N., and Ward, Kenneth E.: Interference of Wing and Fuselage from Tests on 209 Combinations in the NACA Variable-Density Tunnel. NACA Rep. 540, 1935.

17. Jones, R., Williams, D. H., and Bell, A. H.: Experiments on a Model of Rigid Airship R. 29. R.&M. 714, 1921.

18. Freeman, Hugh B.: Force Measurements on a 1/40-Scale Model of the U.S. Airship "Akron." NACA Rep. 432, 1932.

19. Jones, R., and Williams, D. H.: Experiments on a Model of Rigid Airship, R38. British R.&M. 799, A.3.E. Airships 55T1470, May 1920.

20. Trenholm, J. B., and Young, D. W.: Wind Tunnel Tests of Two Prolated Ellipsoids with Fins Differing in Aspect Ratio, Sweep-back, and Dihedral – 1/2 Scale Models of Project MX-570. AAF Tech. Rep. No. 5565, Mar. 25, 1947.

TABLE I.- VOLUMES AND LENGTHS OF THE MODELS

Model	Volume (cu ft)	Length (ft)	Model	Volume (cu ft)	Length (ft)	Model	Volume (cu ft)	Length (ft)
1	4.343	11.33	6	0.520	2.62	11	0.0748	1.68
2	.687	5.04	7	.234	2.62	12	.37	3.47
3	.606	3.36	8	.277	2.62	13	115.00	19.62
4	.509	2.62	9	.0834	2.62	14	.444	4.03
5	.513	2.62	10	.244	2.62	15	1.854	5.00

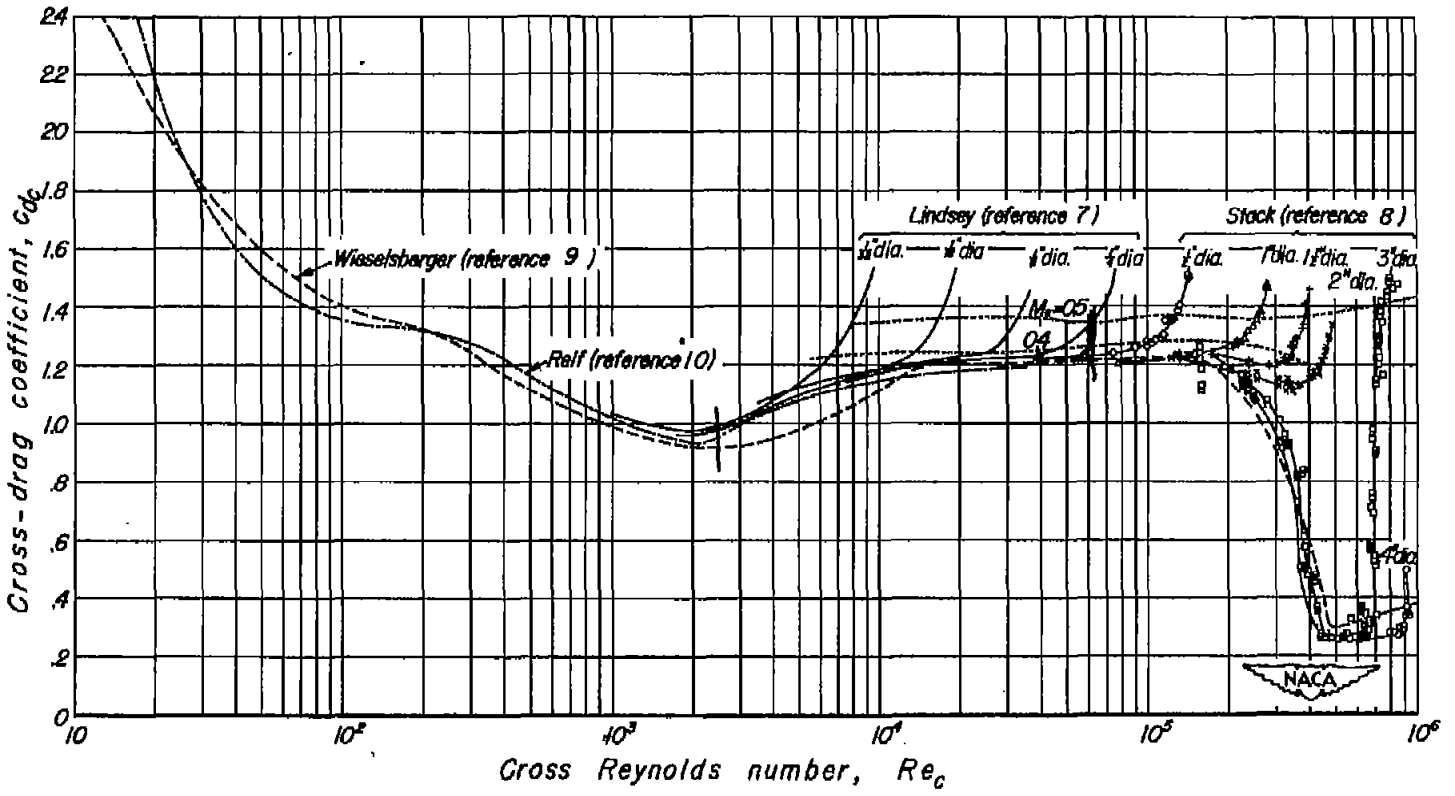

Figure 1.- Circular-cylinder drag coefficient as a function of Reynolds number.

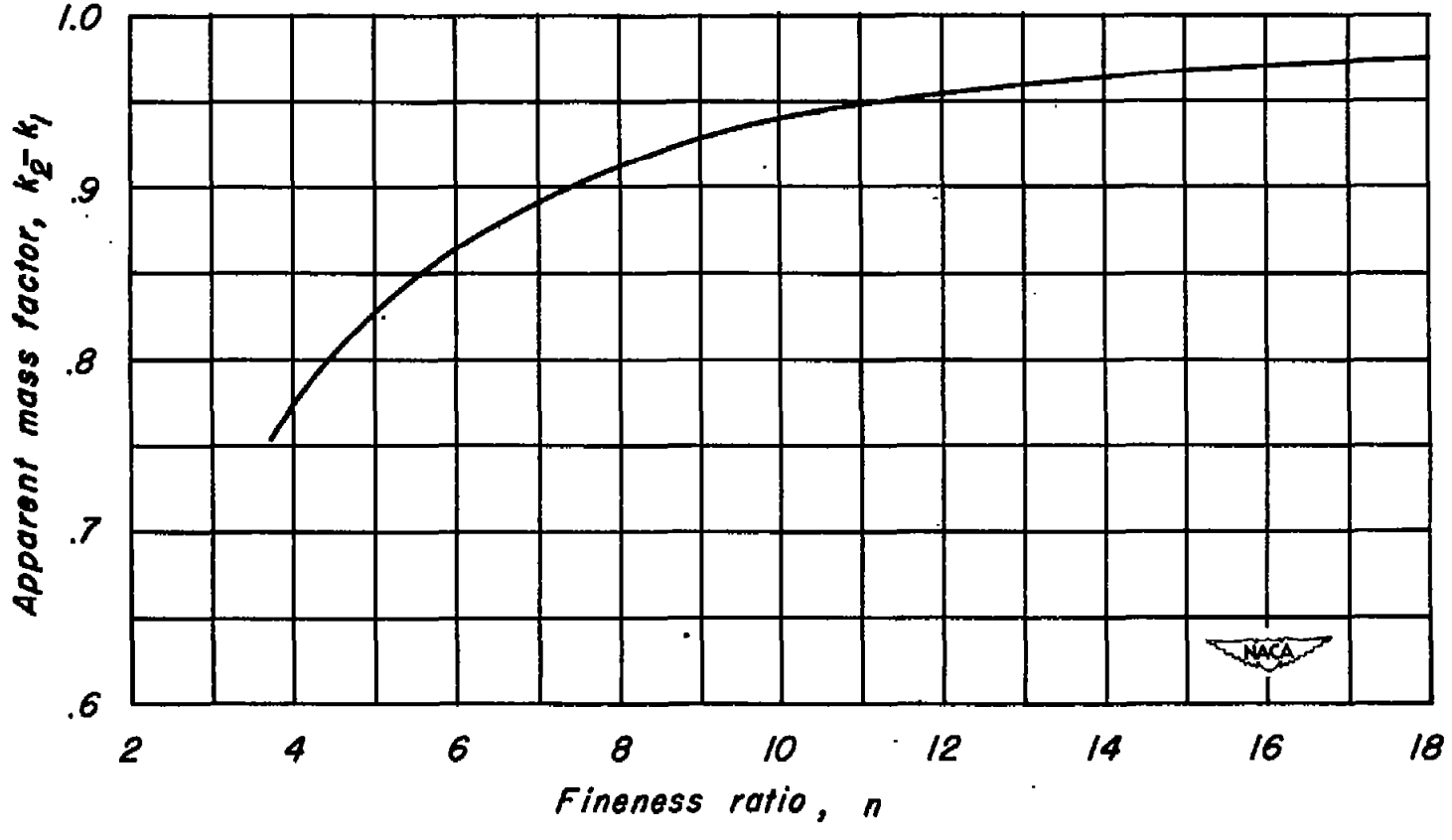

Figure 2.- Apparent mass factor to be used in the calculation of the forces and moments of bodies of revolution.

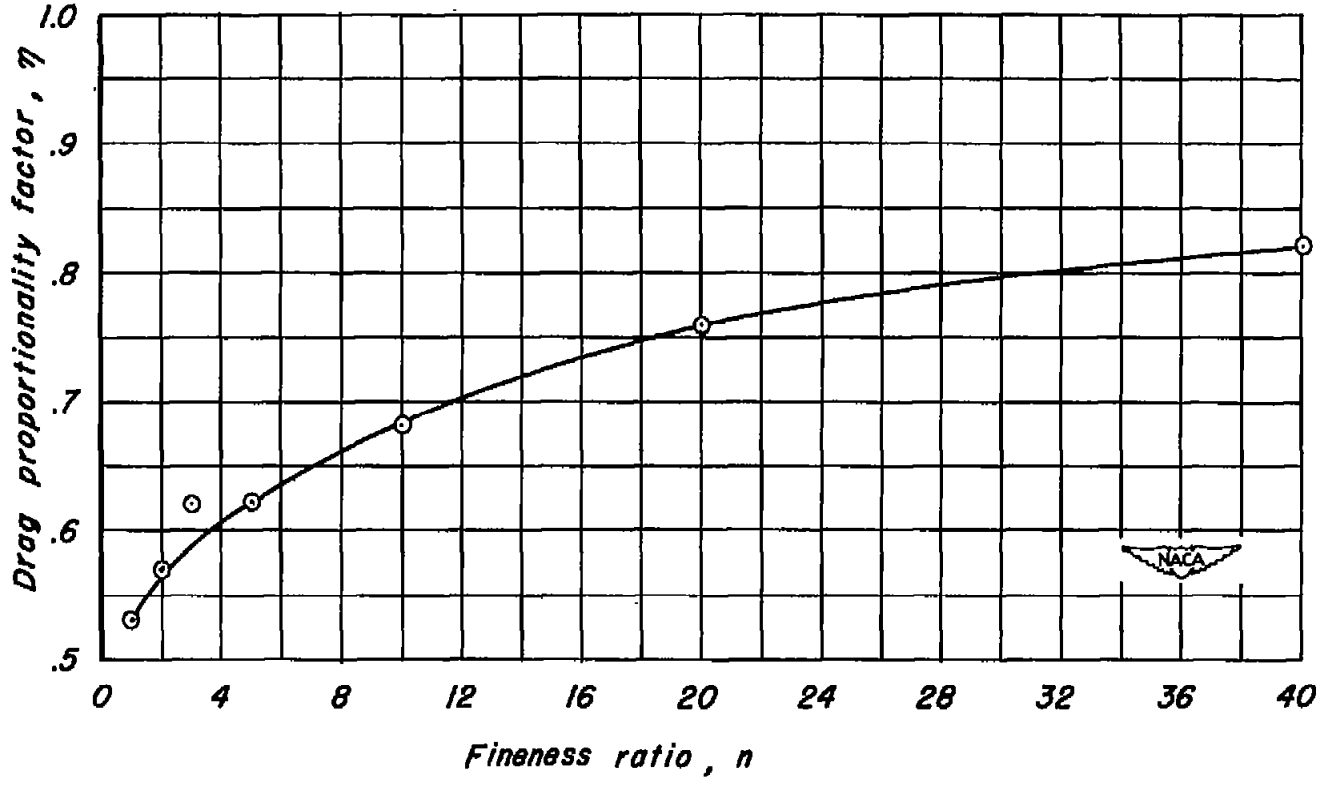

Figure 3.- Ratio of the drag coefficient of a circular cylinder of finite length to that of a cylinder of infinite length as a function of the fineness ratio. R_c=88,000

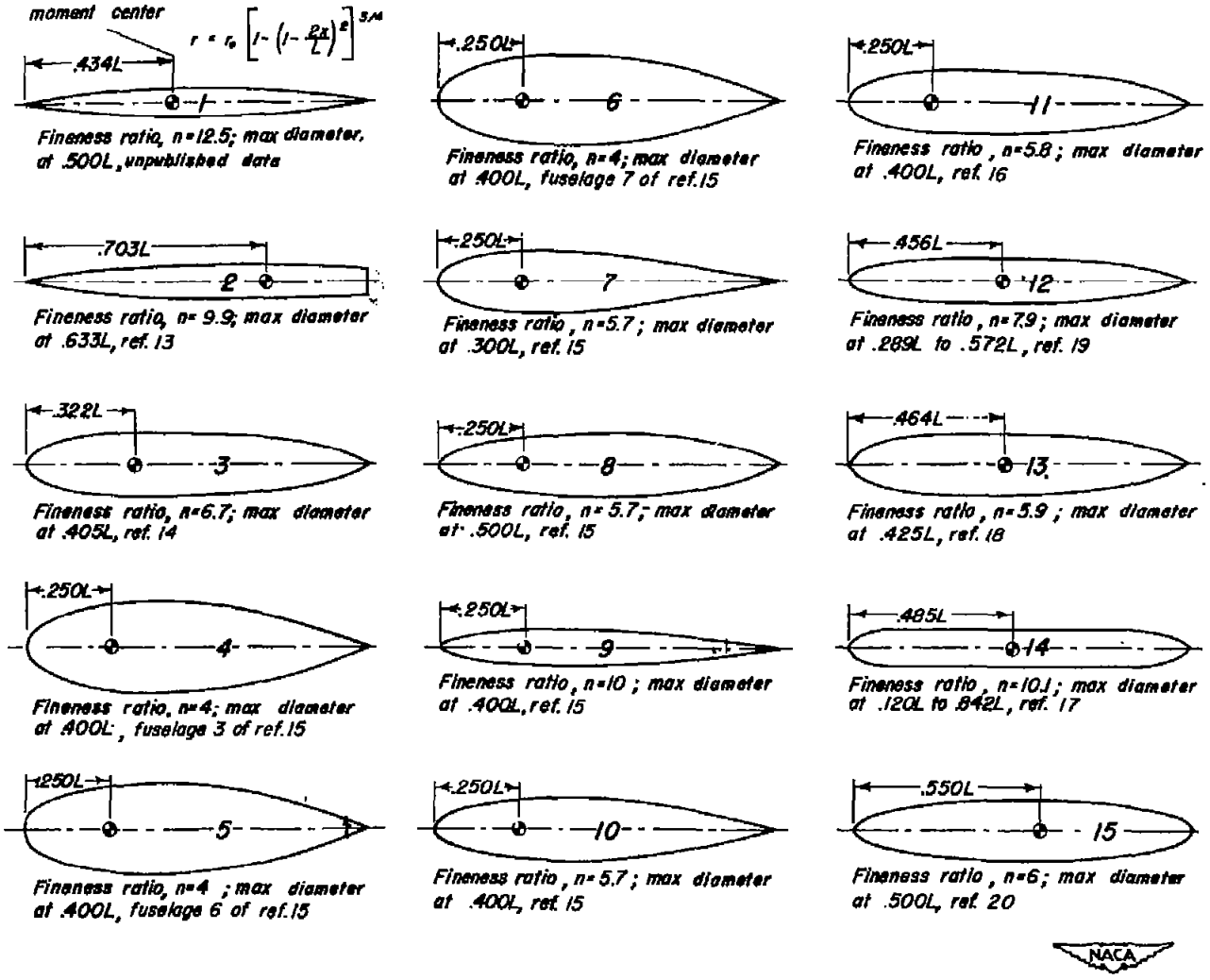

Figure 4.— Model geometry.

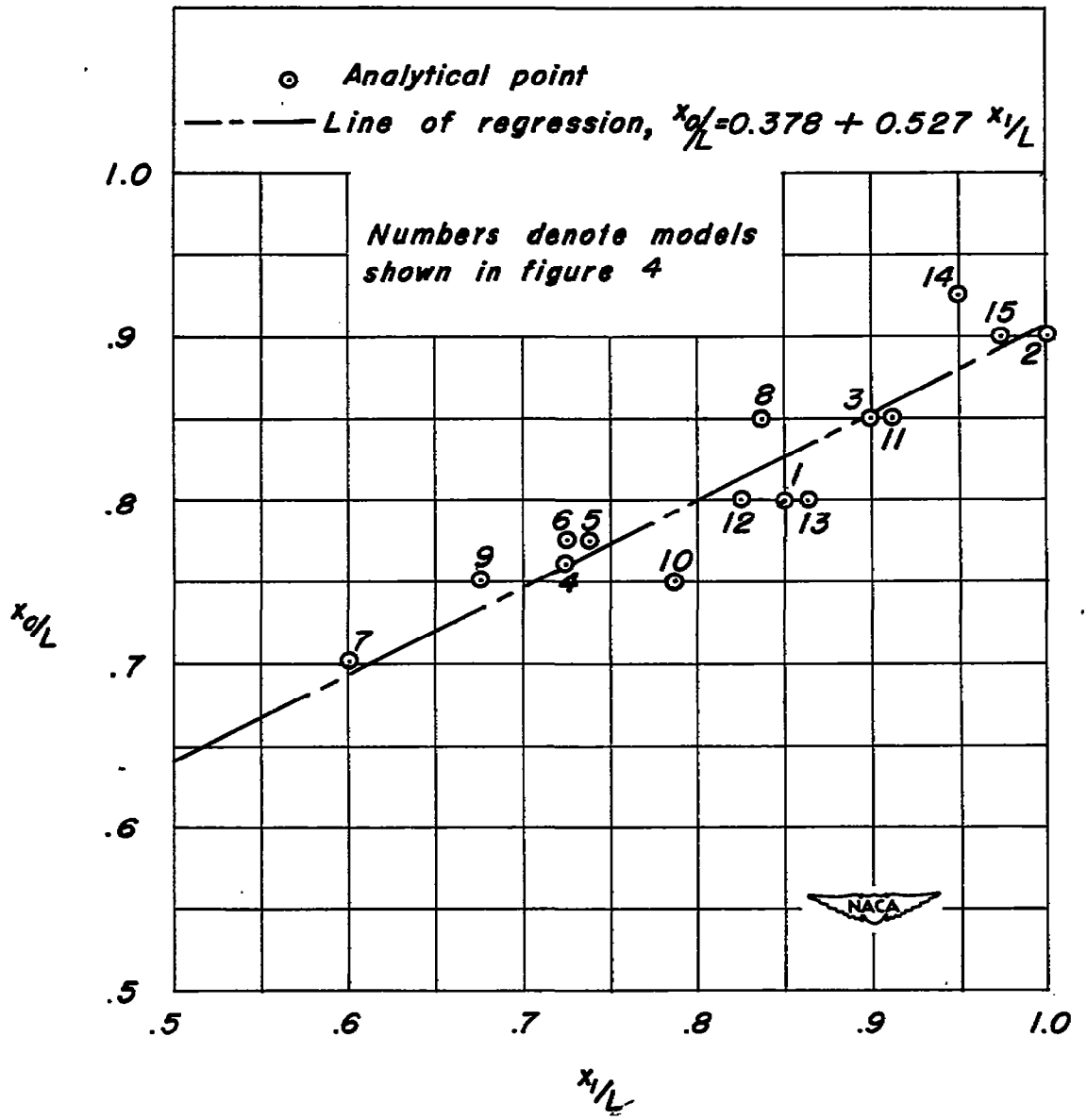

Figure 5.– Correlation between assumed extent of applicability of potential theory and the position of the maximum negative rate of change of body cross-sectional area with body length.

[redacted]

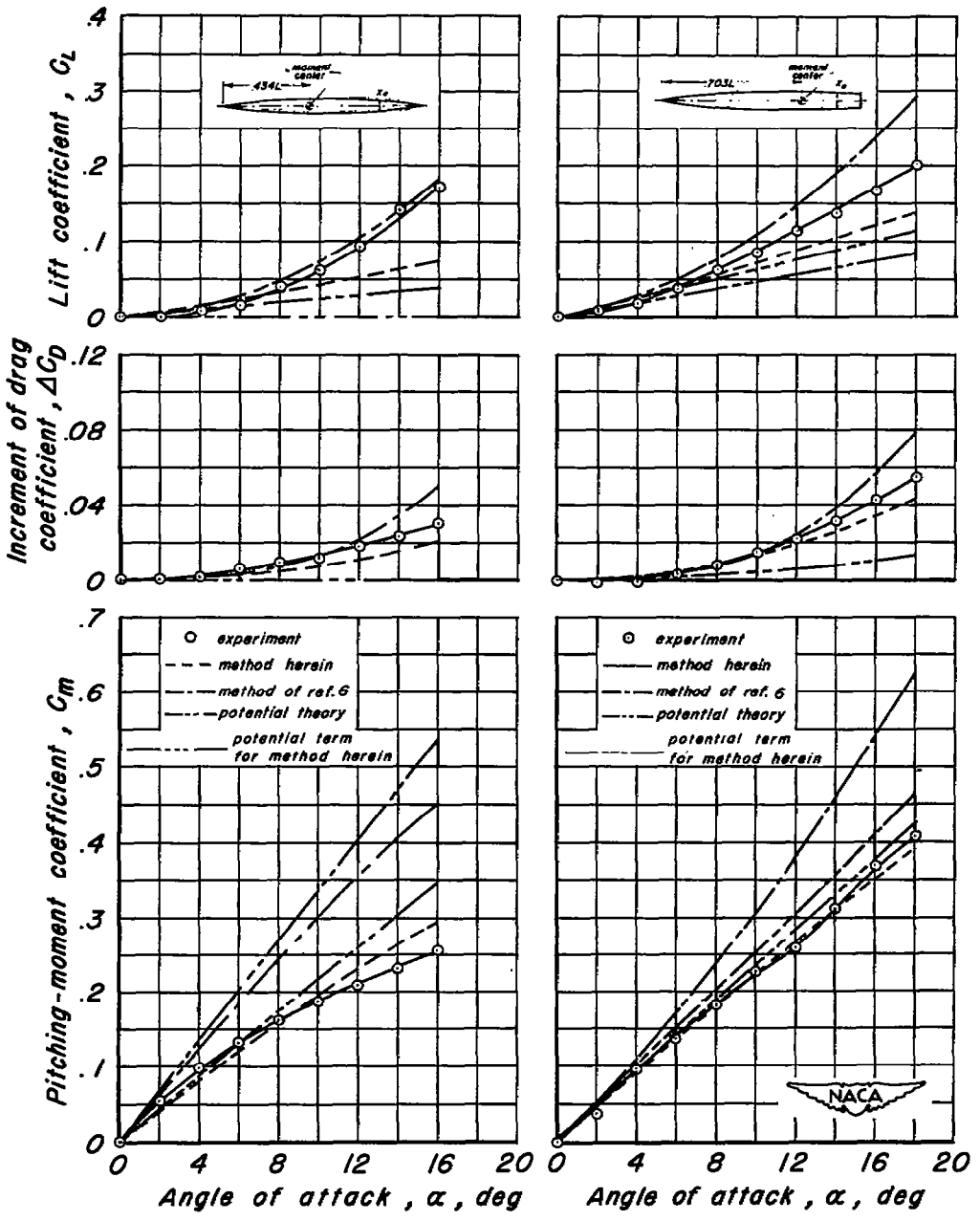

(a) Model 1. (b) Model 2.

Figure 6.- Comparison between the experimental and the estimated lift, drag and pitching-moment characteristics of various bodies of revolution.

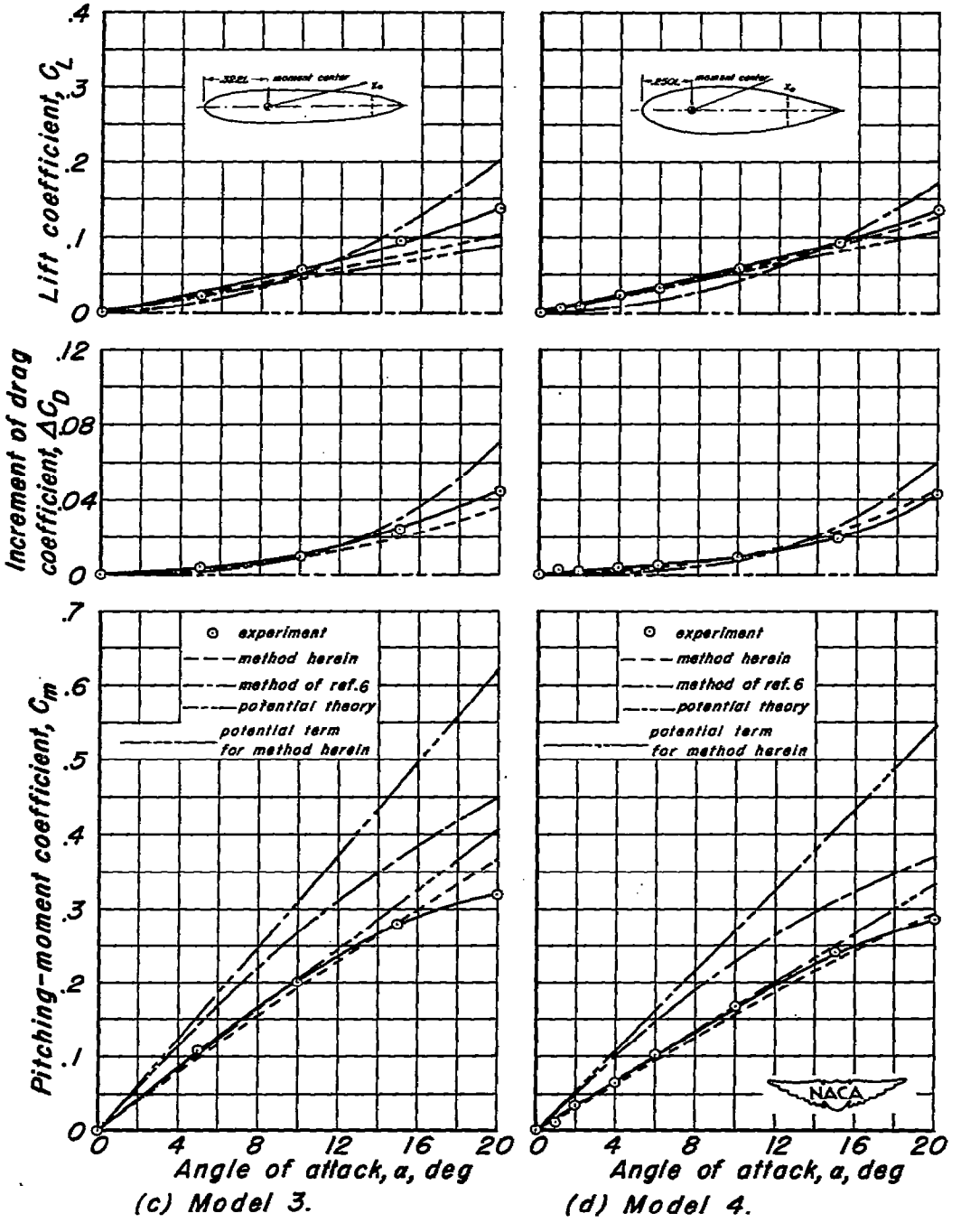

Figure 6.- Continued.

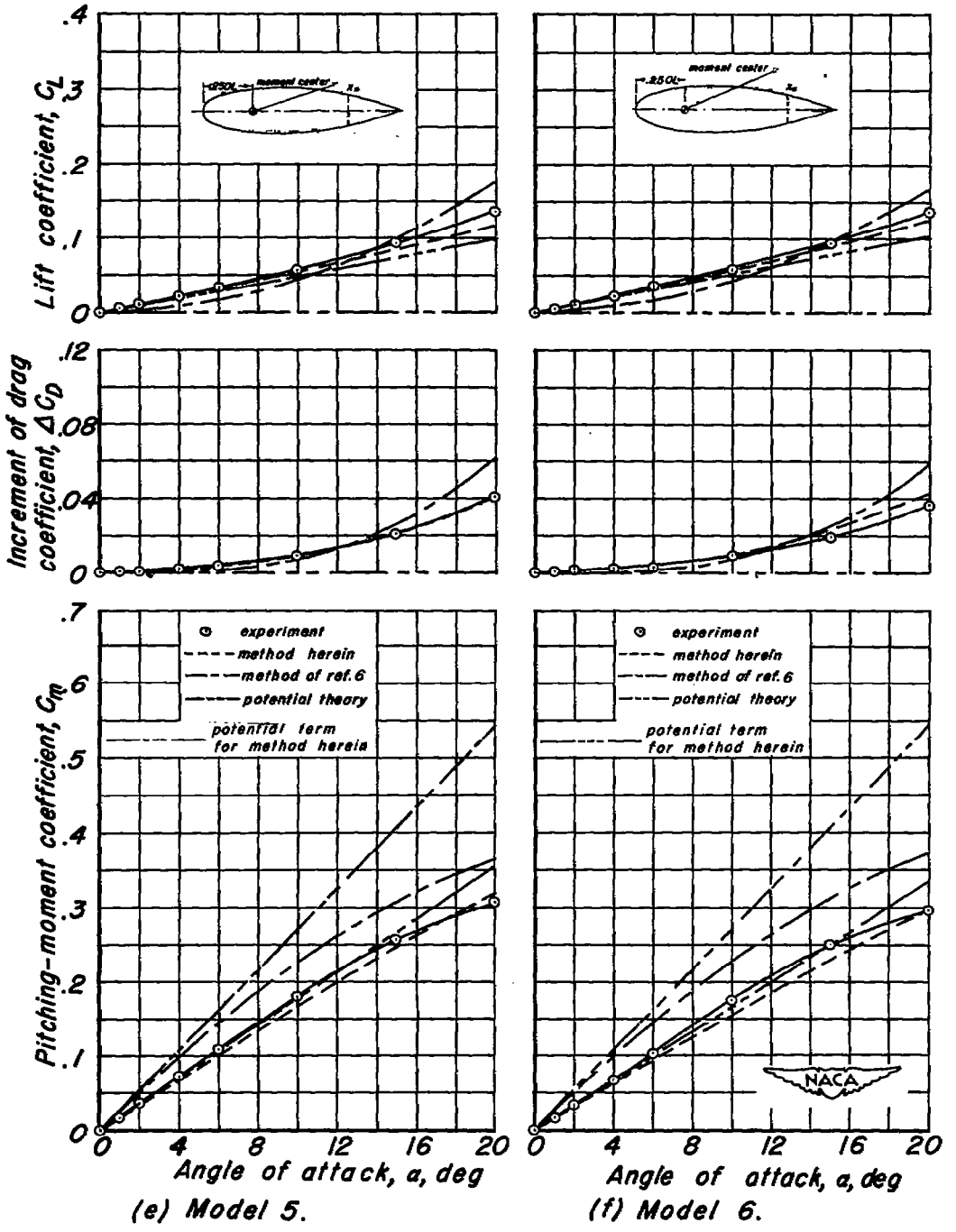

Figure 6.-Continued.

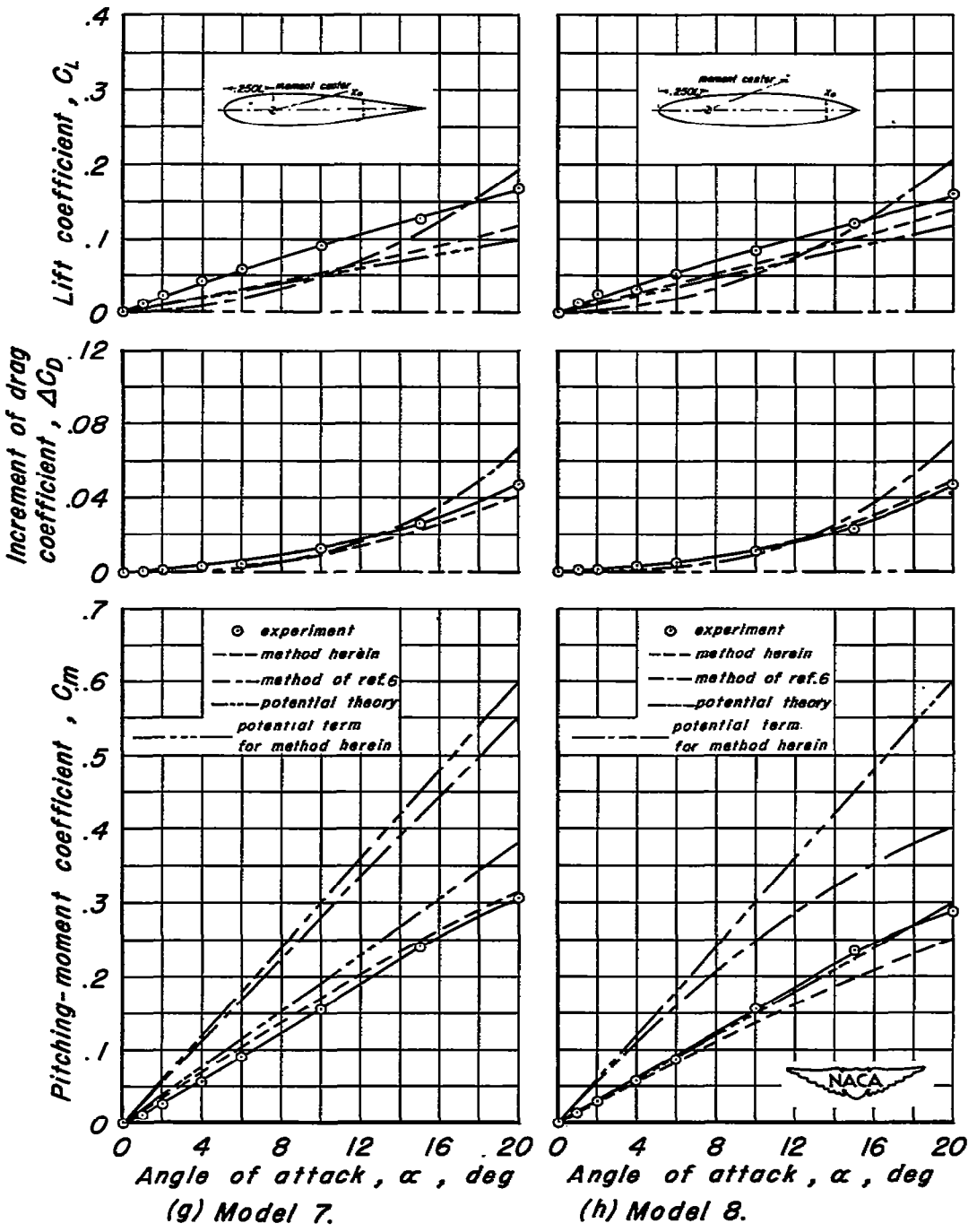

Figure 6.–Continued.

[redacted]

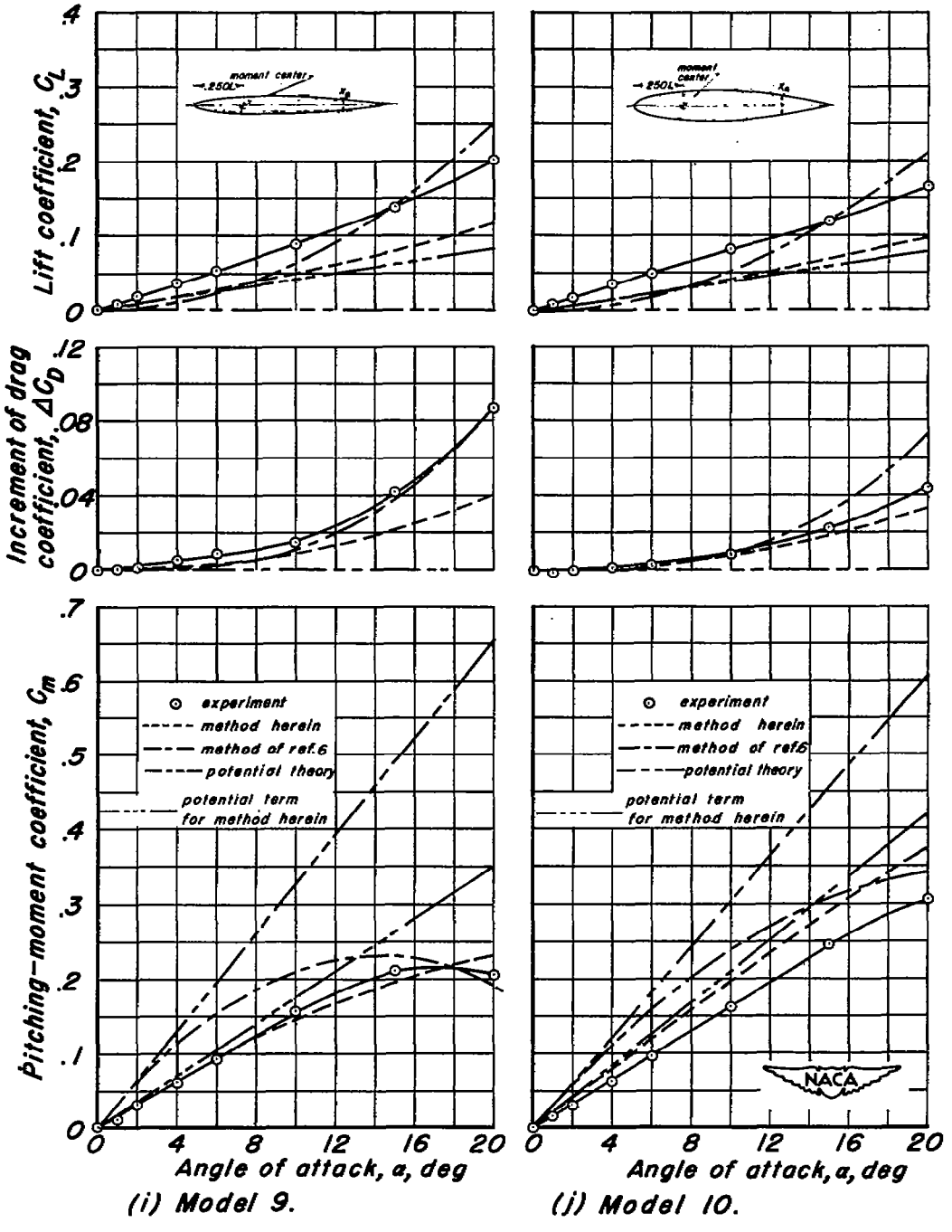

(i) Model 9. (j) Model 10.

Figure 6.- Continued.

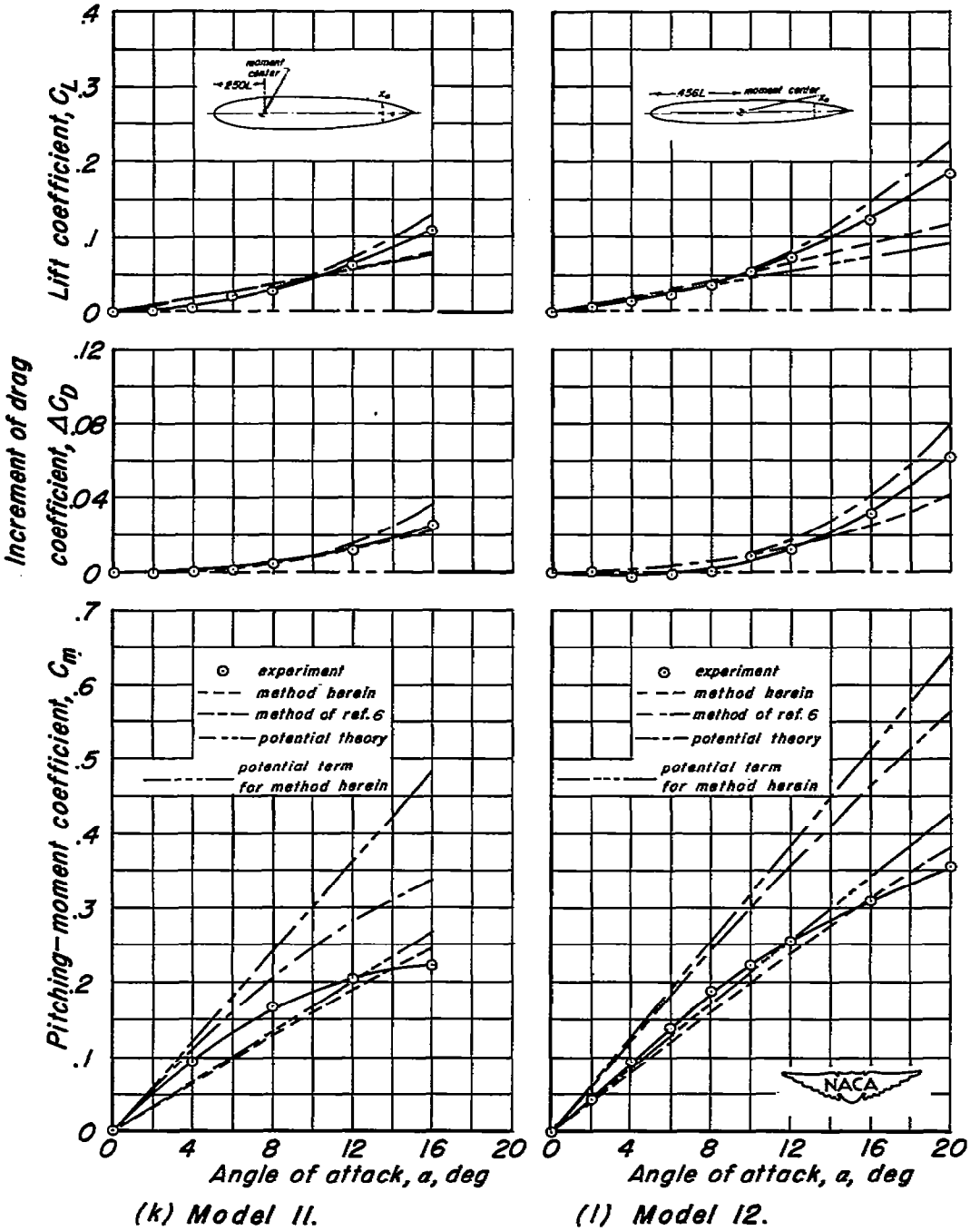

(k) Model 11. (l) Model 12.

Figure 6.- Continued.

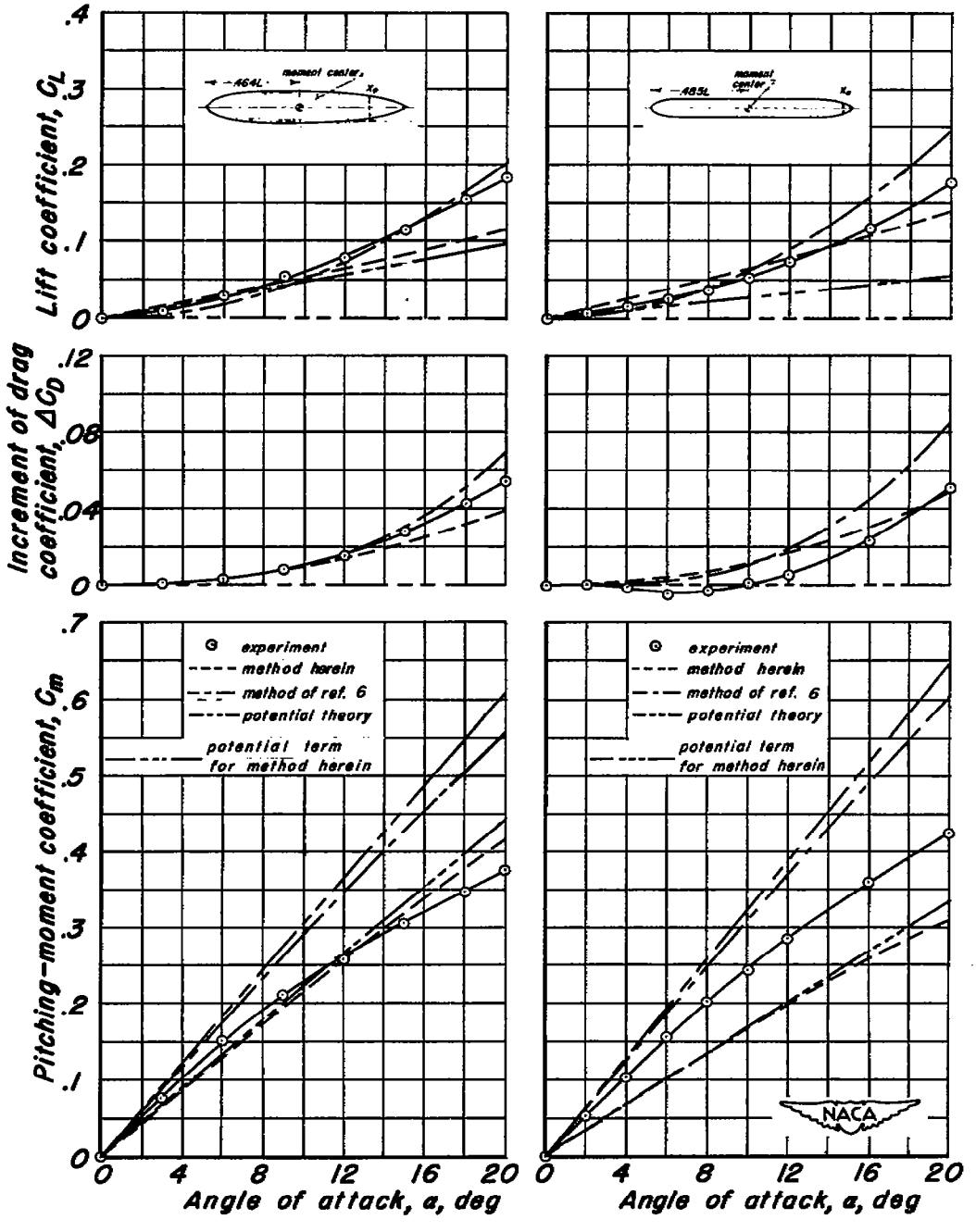

(m) Model 13. (n) Model 14.

Figure 6.-Continued.

[redacted]

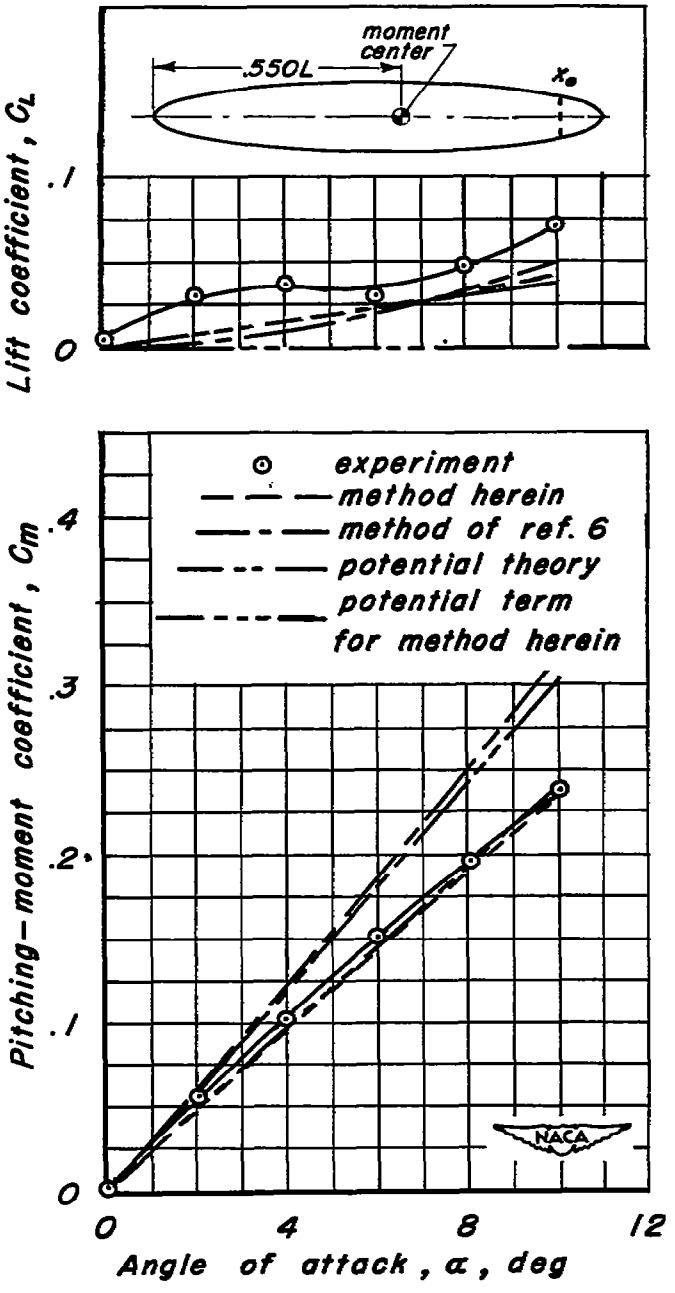

(o) Model 15.

Figure 6.- Concluded.

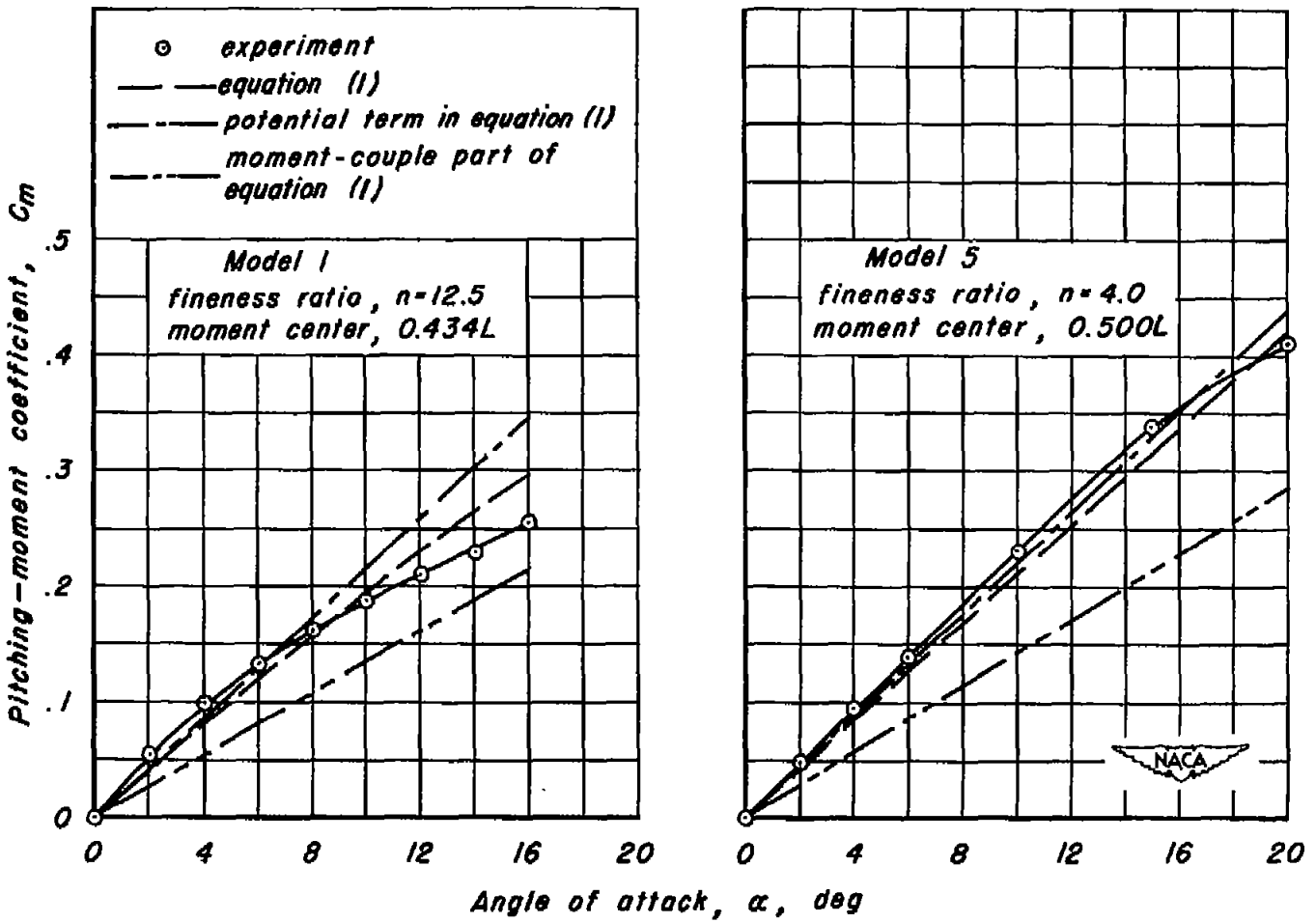

Figure 7.— The components of the pitching-moment coefficient calculated by the method of this report for two different bodies.

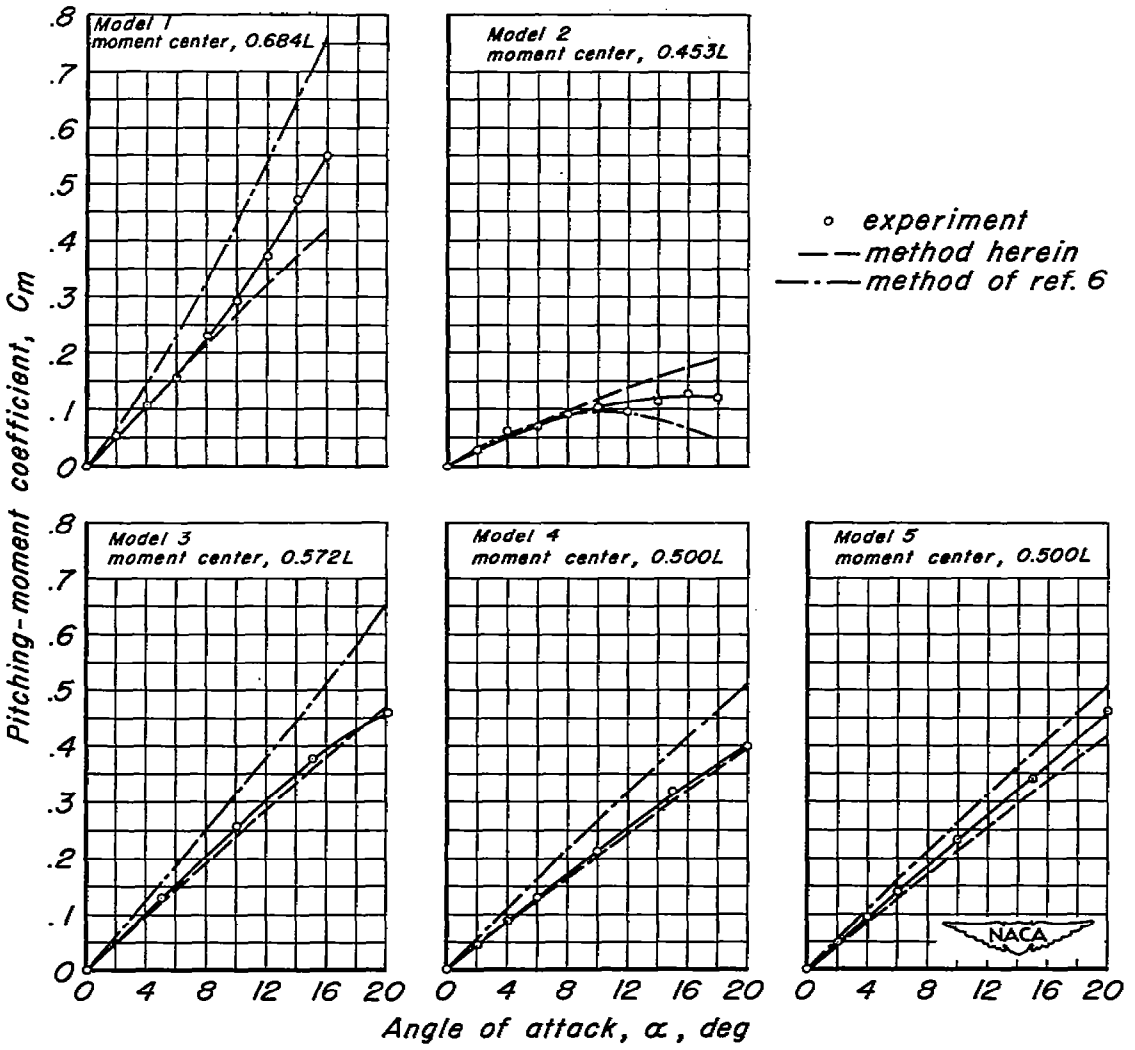

(a) Models 1 to 5.

Figure 8.– Comparison between the experimental and the estimated pitching-moment characteristics of various bodies of revolution.

[redacted]

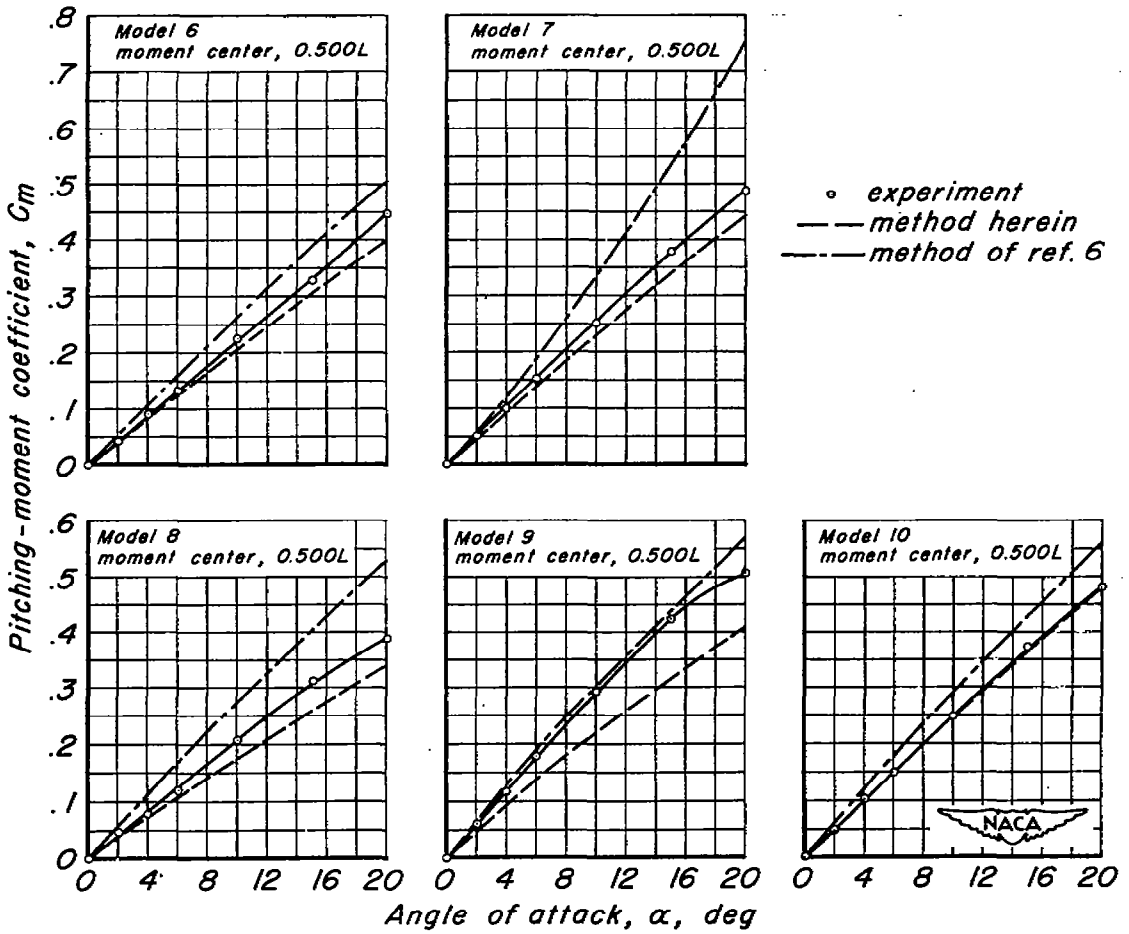

(b) Models 6 to 10.

Figure 8.- Continued.

[redacted]

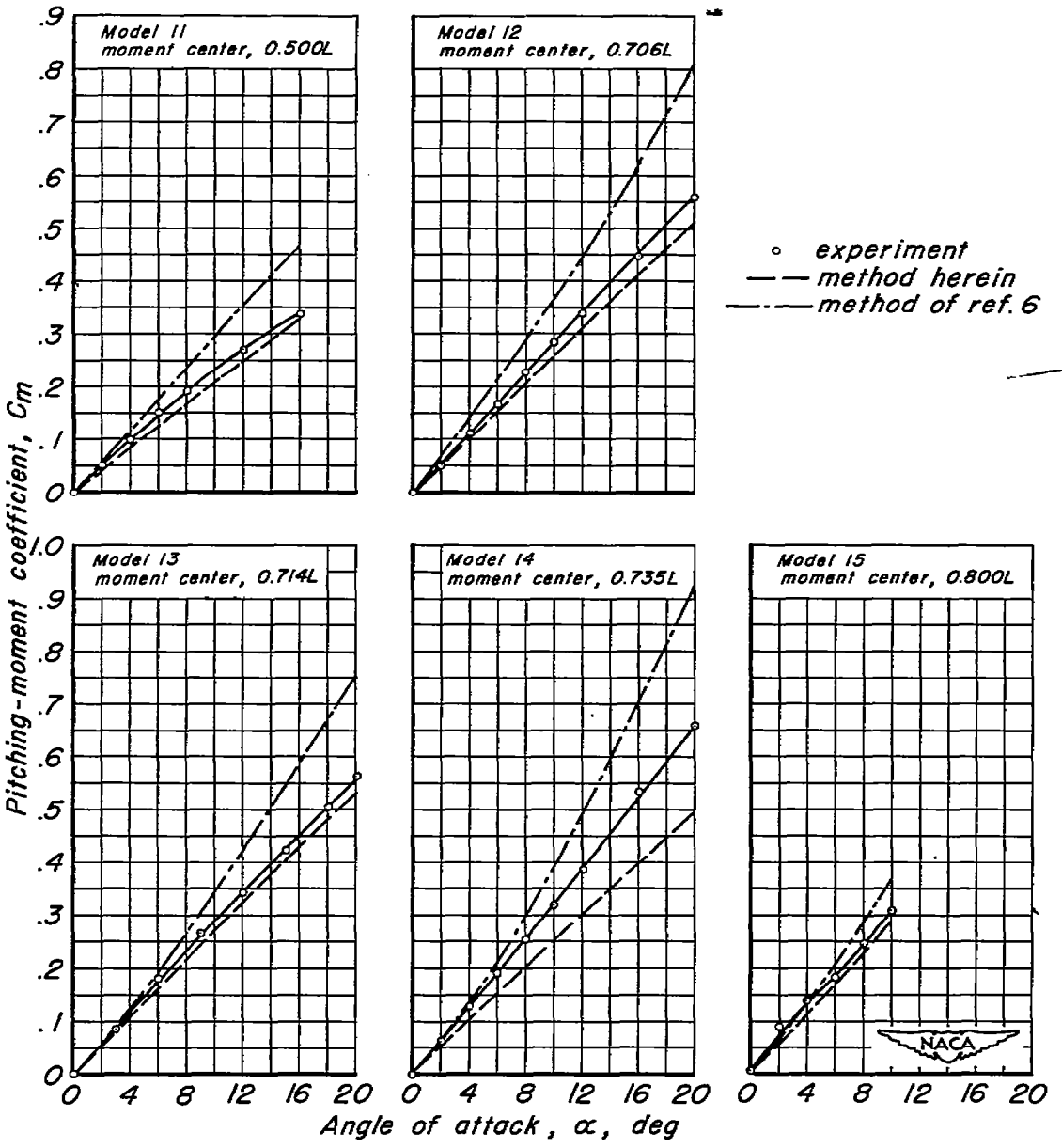

(c) Models 11 to 15.

Figure 8.- Concluded.

[redacted]